MDPI

Review

Recent Progresses on Experimental Investigations of Topological and Dissipative Solitons in Liquid Crystals

Yuan Shen and Ingo Dierking *

Department of Physics and Astronomy, School of Natural Sciences, University of Manchester, Oxford Road, Manchester M13 9PL, UK; yuan.shen@postgrad.manchester.ac.uk
* Correspondence: ingo.dierking@manchester.ac.uk

Abstract: Solitons in liquid crystals have received increasing attention due to their importance in fundamental physical science and potential applications in various fields. The study of solitons in liquid crystals has been carried out for over five decades with various kinds of solitons being reported. Recently, a number of new types of solitons have been observed, among which, many of them exhibit intriguing dynamic behaviors. In this paper, we briefly review the recent progresses on experimental investigations of solitons in liquid crystals.

Keywords: liquid crystal; soliton; toron; skyrmion; nematic; cholesteric; smectic; micro-cargo transport; dissipative dynamics

1. Introduction

Solitons are self-sustained localized packets of waves in nonlinear media that propagate without changing shape. They are found everywhere in our daily life from nerve pluses in our bodies to eyes of storms in the atmosphere and even density waves in galaxies. They were first observed as water waves in a shallow canal by a Scottish engineer John Scott Russell in 1834 [1], which initiated the theoretical work of Rayleigh and Boussinesq and eventually led to the well-known KdV (Korteweg, de Vries) equation which has been broadly used as an approximate description of solitary waves [2]. However, the significance of soliton was not widely appreciated until 1965 when the word "soliton" was coined by Zabusky and Kruskal [3]. Nowadays, solitons have appeared in every branch of physics, such as nonlinear photonics [4], Bose-Einstein condensates [5], superconductors [6], and magnetic materials [7], just to name a few. Generally, solitons appear as self-organized localized waves that preserve their identities after pairwise collisions [8]. This ideal nonlinear property of solitons may enable distortion-free long-distance transport of matter or information and thus makes them considerably attractive to both fundamental research and technological applications [9–11].

Liquid crystals (LCs) are self-organized anisotropic fluids that are thermodynamically intermediate between the isotropic liquid and the crystalline solid, exhibiting the fluidity of liquids as well as the order of crystals [12,13]. Generally, LCs consist of anisotropic building blocks with rod- or disc-like shapes, which spontaneously orient in a specific direction on average, called director, **n**. As a typical nonlinear material, LCs have been broadly used as an ideal testbed for studying solitons, in which different kinds of solitons have been generated in the past five decades.

In this review, we first give a brief overview of the early works of solitons in LCs (Section 2), which is followed by a short discussion of investigations on nematicons (Section 3) and a discussion of recent progress in studies of topological solitons in chiral nematics (Section 4). The article then continues by overviewing the investigations of dynamic particle-like dissipative solitons, "director bullets" or "directrons", which were first reported by Brand et al. in 1997 but did not receive much attention until recently

(Section 5). This review is mainly focused on the recent experimental investigations on solitons in liquid crystals, readers who are interested in this topic can find more detailed early experimental and theoretical investigations in the excellent book edited by Lam and Prost [14].

2. Early Works

The study of solitons in LCs was started in 1968 by Wolfgang Helfrich [15]. He theoretically modelled alignment inversion walls as static solitons in an infinite sample of nematic order. By applying a magnetic field, **H**, depending on the assumed orientation of the director at infinity, there are three types of possible walls, i.e., twist wall, splay-bend wall parallel to the applied field, and the splay-bend wall perpendicular to the field, which are analogous to the Bloch and Neel walls in ferromagnetics (Figure 1). Such a model was later improved by de Gennes who studied the boundary effects of the substrate and the movement of the walls [16].
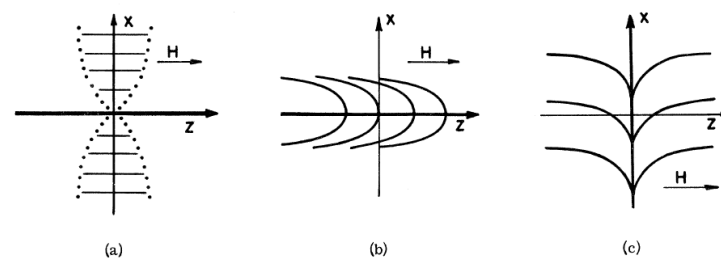
Figure 1. Schematic diagrams of different alignment inversion walls. (**a**) Twist wall. (**b**) Splay-bend wall parallel to the magnetic field. (**c**) Splay-bend wall vertical to the magnetic field. Reprinted with permission from Ref. [15]. Copyright 1968 American Physical Society.

The first experimental investigation of these inversion walls was probably reported by Leger in 1972 [17]. In this work, a 180° twist wall was generated at the top free surface of a nematic droplet by rotating the applied magnetic field by 180° (Figure 2a,b). The migration time of the twist walls was also measured. However, instead of working with a free surface geometry, the measurements were carried out in nematic droplets sandwiched between two rubbed glass plates due to the difficulty of measuring the sample thickness. In this case, the twist walls were generated near each glass plate and then moved toward the midplane of the sample. Because the pair had opposite twists, they annihilated each other once they met. The measured migration time was in great agreement with theoretical prediction [16]. However, because the observation was from the top of the sample, one could not really see the propagation process of the twist walls in the experiment.

In the same year, a different type of wall was investigated theoretically by Brochard [18] and experimentally by Leger [19,20]. These walls separate domains in which LC molecules rotate in two different directions, i.e., the so-called reverse tilt domains [21]. They can be generated by increasing the applied magnetic field above the Freedericksz transition (Figure 2c,d). The walls can either form in a straight line state where they are stable and static or in a closed loop state where they continuously shrink inward and eventually annihilate to minimize the free energy. The authors investigated the static structure and the dynamic behavior of the walls. Unlike the twist walls mentioned above, the walls discussed here move in the plane of the LC cell and can be observed directly.
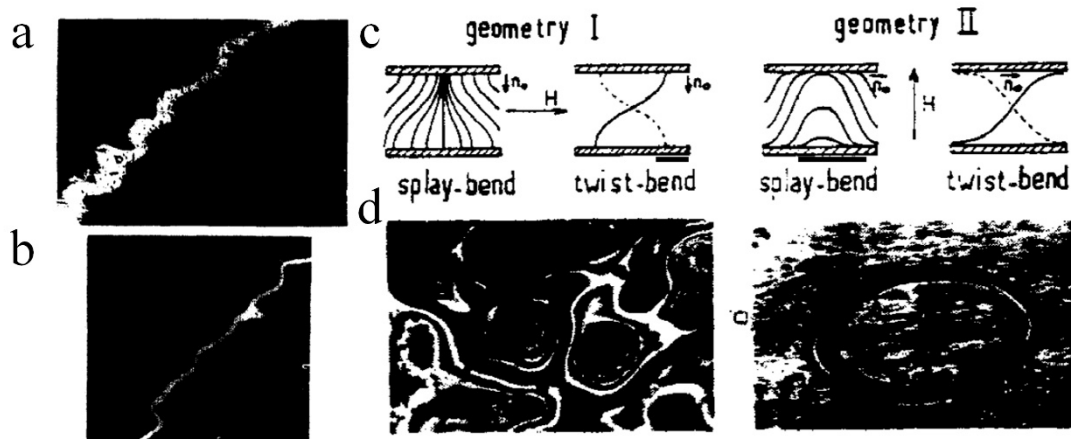
Figure 2. Typical image of the free surface of a MBBA droplet within which a twist wall was generated at (**a**) H = 3000 G and (**b**) H = 6000 G, where H represents the magnitude of the magnetic field. Reprinted with permission from Ref. [17]. Copyright 1972 Elsevier. (**c**) Schematic distortion of the director structure of different walls. (**d**) The microscopy of the walls corresponding to (**c**). Reprinted with permission from Ref. [19]. Copyright 1972 Elsevier.

The interactions between flows and director field in a nematic LC can introduce a nonlinear term in the director equation of motion. Thus, it is possible to induce solitons by shearing nematics without applying any external field [14]. In 1976, Cladis and Torza reported propagating solitary wave instabilities of a nematic in a Couette flow field [22]. They found that for small shears, a "tumbling" instability was observed, which was similar to the appearance of a solitary wave in a long torsion bar to which is attached a dense array of pendulums. By slightly increasing the shear rate, a cellular flow instability was induced (Figure 3a). Further increase of the shear rate, led to a dense mass of disclinations being formed, which aligned with their long axis parallel to the flow field. At very large shear rates, Taylor vortices were generated. In 1982, Zhu reported a soliton-like director wave in a nematic by mechanical shearing [23]. In his work, the nematic film was confined in a home-made cell with an exciter at the entrance. The nematic was homeotropically aligned. By moving the exciter, propagating director waves were observed through polarized white light as black lines, which travelled through the nematic bulk (Figure 3b). It should be noted that these solitons were first theoretically predicted and explained by Lin et al. [24–26]. Later, in 1987, C. Q. Shu et al. reported the generation of two-dimensional (2D) axisymmetric propagating solitons in a radial Poiseuille flow of homeotropic nematic LCs [27]. These solitons appear as dark rings in polarized white light and are large enough to be observed directly by the naked eye (Figure 3c). They are generated by periodically pressing the rim of the cell and can move through the nematic bulk at a constant speed with their shape remaining unchanged.

Convection as one of the simplest examples of hydrodynamic instability induces a rich variety of nonlinear phenomena in a fluid. In conventional Rayleigh-Benard and Taylor experiments, convective patterns emerge once the temperature gradient across the fluid layer, and the relative velocity field of the rotating planes, exceed some specific threshold (the Rayleigh number R_a and T_a). Generally, the convective pattern is composed of spatially periodic rolls (Williams rolls) with translational invariance, whose periodicity is of order of the thickness of the fluid layer. In LCs, the convective pattern exhibits similar characteristic features and can be generated by applying an electric field to a properly aligned nematic. It was reported that the nonlinear coupling between the convective flow and the director field may lead to the generation of a number of solitonic structures. In 1979, Ribotta measured the penetration length of a vortex into a subcritical region by using the electro-convective instability in a nematic LC [28]. In his experiment, the electrode on one plate is divided into two parts separated by a small gap of about 5 μm. Convective patterns are generated in one

region (region 1) by applying an electric field. An electric field with the same frequency but a relatively low amplitude is applied in the other region (region 2), in which no convective pattern is generated. One then observes that small portions of individual rolls are "emitted" from the gap, and propagate into region 2 with a uniform group velocity (Figure 4a). The rolls behave like solitary waves with their shape and amplitude remaining constant during the motion. A different kind of soliton was later reported by Lowe and Gollub in 1985 in a convecting nematic subjected to spatially periodic forcing [29]. The solitons (also called domain walls or discommensurations) are regions of local compression of convective rolls (Figure 4b) and can be well described by the solutions to the Sine-Gordon equation. Generally, the convective pattern is stationary and spatially homogeneous with its velocity field and orientational field being time independent. However, in 1988, Joets and Ribotta reported a time-dependent localized state of electro-convection in a nematic [30]. These spatially localized domains exhibit elliptical shape and distribute randomly throughout the sample. Inside the domains, a periodic structure of Williams Rolls translates uniformly (Figure 4c). The velocity of the rolls has the same amplitude in different domains, but its sign changes randomly from one domain to another. The domains themselves do not show uniform translational motion, instead they fluctuate around an average location. Both the velocity of the rolls and the shape of the domains can be varied by tuning the applied electric field.
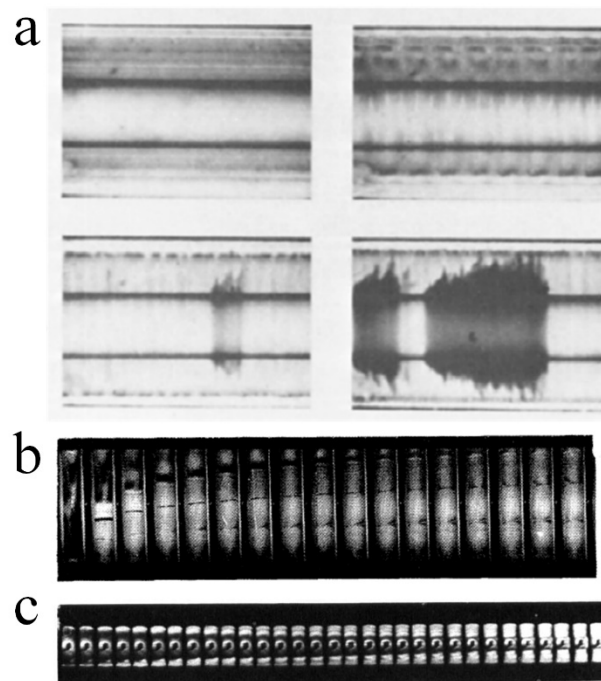

Figure 3. (**a**) Cellular flow in a nematic LC. Reprinted with permission from Ref. [22]. Copyright 1976 Elsevier. (**b**) Propagation process of the director wave. Reprinted with permission from Ref. [23]. Copyright 1982 American Physical Society. (**c**) Propagation of the 2D axisymmetric soliton. Reprinted with permission from Ref. [27]. Copyright 1987 Taylor & Francis.
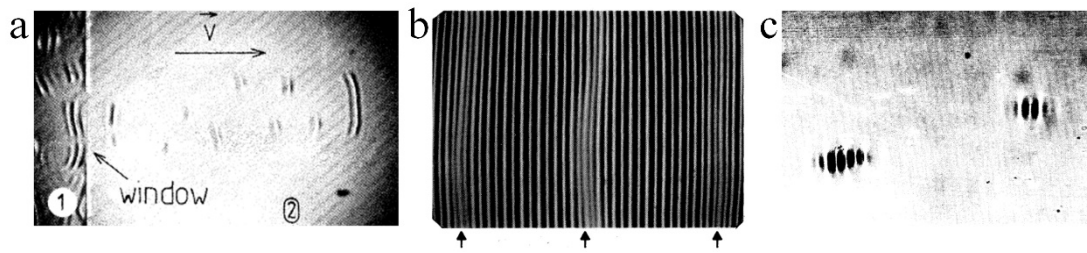
Figure 4. (**a**) Portions of convective rolls "emitted" from region 1 to region 2. Reprinted with permission from Ref. [28]. Copyright 1979 American Physical Society. (**b**) Micrograph of a quasiperiodic convective structure. The solitons (indicated by arrows) are regions of compression of the rolls. Reprinted with permission from Ref. [29]. Copyright 1985 American Physical Society. (**c**) Micrograph of localized domains of travelling convective rolls. Reprinted with permission from Ref. [31]. Copyright 1988 American Physical Society.

3. Nematicons

Nematicons are self-focused light beams (spatial optical solitons) that propagate in nematic LCs. The beginning may date back to the early works by Braun et al. in which optical beams of complex structures, such as the formation of focal light spots, the onset of transverse beam undulations, and the development of multiple beam filaments, are realized by interacting a low-power laser beam with a nematic LC [32,33]. Compared to most materials, the nonlinear coefficient of nematic LC is extremely large (10^6 to 10^{10} times greater than that of typical optical materials such as CS_2), making it an ideal system for investigating spatial optical solitons [32]. As shown in Figure 5, a linearly polarized beam propagates along the z-axis and enters a nematic cell. The polarization of the beam is parallel to the y-axis. The nematic LC within the cell is homogeneously aligned with its director, **n**, being parallel to the cell substrates but making an angle θ with respect to the wave vector (**k**) of the beam. The extraordinary waves of the beam whose electric field **E** is in the **nk** plane propagate along the Poynting vector **S** which is deviated from **k** at the angle δ [34]. The light induces electric dipoles in the LC molecules which interact with the electric field and produce a torque $\Gamma = \varepsilon_0 \Delta\varepsilon (\mathbf{n} \cdot \mathbf{E})(\mathbf{n} \times \mathbf{E})$, where ε_0 is the dielectric susceptibility of vacuum, $\Delta\varepsilon = n_e^2 - n_o^2$ is the optical anisotropy, n_e and n_o are the extraordinary and ordinary refractive indices, respectively. For nematic LCs with $n_e > n_o$, the torque reorients the director and increases the angle θ, leading to the increase of the extraordinary refractive index $n_{e,\theta} = \frac{n_e n_o}{\sqrt{n_o^2 \cdot \sin^2(\theta) + n_e^2 \cdot \cos^2(\theta)}}$. Such an increase of the refractive index focuses the beam, and leads to the formation of a nematicon which propagates along **S**. The study of nematicons has attracted a great deal of interest since the beginning of the 21st century due to its promising applications in nonlinear optics and photonics [35]. Recently, different kinds of nematicons, such as vortex nematicons [36–38], have been reported. Since this review is mainly concentrated on topological and dissipative LC solitons, we refer the readers who are interested in nematicons, to a book and several reviews published by Assanto, et al., recommended here [35,39–41].
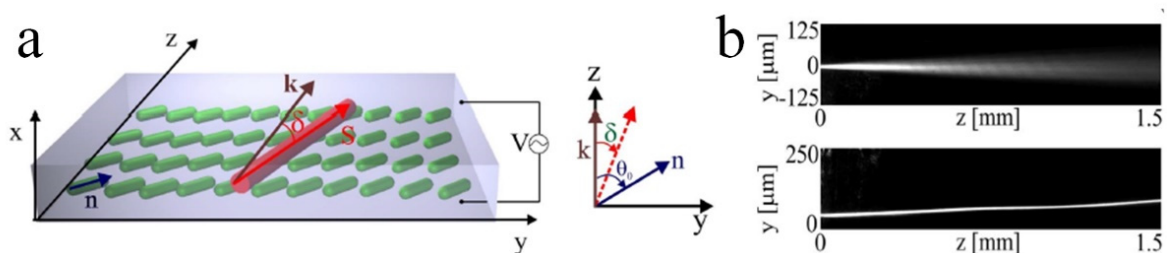
Figure 5. (**a**) Schematic of the formation of a nematicon in a planar nematic LC cell. (**b**) Photographs of a propagating ordinary light beam (top) and a nematicon (bottom). Reprinted with permission from Ref. [34]. Copyright 2019 Optical Society of America.

4. Topological Solitons in Chiral Nematics

Topological solitons are continuous but topologically nontrivial field configurations embedded in uniform physical fields that behave like particles and cannot be transformed into a uniform state through smooth deformations [42]. They were probably first proposed by the great mathematician Carl Friedrich Gauss, who envisaged that localized knots of physical fields, such as electric or magnetic fields, could behave like particles [43]. Kelvin and Tait noticed the importance of this concept in physics and proposed one of the early models of atoms, in which they tried to explain the diversity of chemical elements as different knotted vortices [43]. Based on these theories, Hopf proposed the celebrated mathematical Hopf fibration [44], which was later applied to three-dimensional physical fields by Finkelstein [45] and led to the increasing interest of topological solitons to mathematicians and physicists. Nowadays, topological solitons have been investigated in many branches of physics such as instantons in quantum theory [46,47], vortices in superconductors [48], rotons in Bose-Einstein condensates [49], and Skyrme solitons in particle physics [50], etc. The field of topological solitons in LCs started about 50 years ago with the discussion of static linear and planar solitons, which are actually the inversion walls discussed above. In this section, the attention will be mainly focused on the 3D particle-like topological solitons, i.e., the so-called "baby skyrmions", in chiral nematic LCs (CNLCs).

In CNLCs, topological solitons such as 2D merons and skyrmions (low-dimensional analogs of Skyrme solitons) can be generated and have recently received great attention. The molecules of a CNLC form a "layered" structure. In each molecular layer, the director, **n**, aligns in a specific direction. The director of different layers twists at a constant rate along a helical axis which is perpendicular to the layers. The distance over which **n** rotates by an angle of 2π is called the pitch, *p*. Generally, by applying an electric field to a CNLC or sandwiching it between surfaces of homeotropic anchoring, the helical superstructure of the CNLC will be deformed, leading to the formation of string-like cholesteric fingers [51] and/or nonsingular solitonic field configurations [52]. In 1974, Haas and Adams [52] reported the formation of densely packed particle-like director field configurations, called "spherulites" by the authors, which are now known as "skyrmions", following Skyrme who developed a 3D soliton model of nucleons [50]. In the experiment, the CNLC is confined in a cell with homeotropic anchoring. By applying an electric field to the sample, electro-hydrodynamic effects are induced, and the spherulites can be generated after removing the electric field. Almost at the same time, similar results were also reported by Kawachi et al. [53]. However, in their publication, the spherulites were called "bubble domains". These spherulites or bubble domains soon attracted a great deal of interest and fueled an explosive growth of studies in the next few years [54–62]. In 2009, with the help of laser tweezers, different kinds of spherulites or bubble domains were optically generated at will at a selected place of a homeotropically aligned CNLC by Smalyukh, et al. [63]. By characterizing and simulating the 3D director structure of these solitons, the authors recognized that these are low-dimensional analogs of Skyrme solitons. The solitons are composed of a double-twist cylinder closed on itself in the form of a torus and coupled to the surrounding uniform field by point or line topological defects and are called "torons" (Figure 6a). The authors successfully demonstrated the structure and stability of the torons by the basic field theory of elastic director deformations and obtained the equilibrium field configuration and elastic energy of torons through numerical simulations. Later, the same authors reported the generation of 2D reconfigurable photonic structures composed of ensembles of torons [64–66]. In 2013, Chen et al. reported the generation of Hopf fibration (Figure 6c) in a CNLC by manipulating the two point defects of torons [67]. They demonstrate the relationship between Hopf fibration and torons through a topological visualization technique derived from the Pontryagin-Thom construction. In the following years, a variety of different kinds of skyrmionic solitons, such as half-skyrmions, twistion, skyrmion bags, skyrmion spin ice, skyrmion-dressed colloidal particles, and more complicated structures composed of torons, hopfions, and various

disclinations, were realized and reported by different groups [68–76]. The self-assembly of torons (Figure 6d) [77–79] and hopfions in ferromagnetic LCs were later realized by Ackerman et al. [80]. Furthermore, the continuous transformation of 3D Hopf solitons [81] and the generation of 3D knots dubbed "heliknotons" (Figure 6e,f) [82] in CNLCs were reported by Tai et al. Due to the continuous twist of the director field within topological solitons, they can be used as optical devices for controlling and modulating the propagation of light [83–86]. For instance, Varanytsia et al. reported that the surface-assisted assembly of a two-dimensional toron array could be utilized as a spatial light modulator to control the light transmission and scattering [83,87]. Recently, Hess et al. showed that the skyrmionic solitons can act as lenses to steer laser beams [84]. Papic et al. showed that the topological LC solitons inserted in a Fabry-Perot microcavity can be used as a tunable microlaser to generate structured laser beams. The structure of the emitted light could be easily controlled by tuning the topology and geometry of the solitons [88]. In addition, Mai et al. recently showed that topological solitons, such as heliknotons, can be used as micro-templates for spatial reorganization of nanoparticles [89].
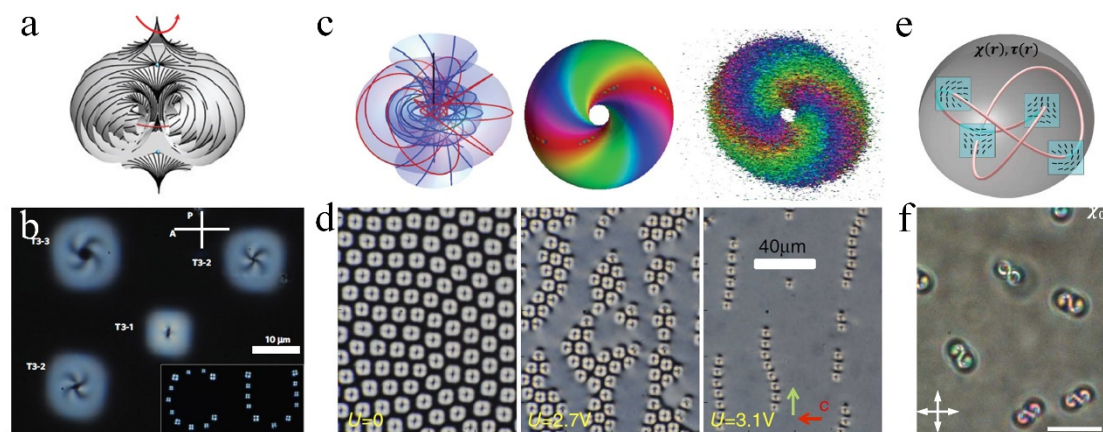
Figure 6. (**a**) Configuration of a toron. (**b**) Polarizing microscopy texture of different defect-proliferated torons. Reprinted with permission from Ref. [63]. Copyright 2010 Nature. (**c**) Flow lines and preimage surfaces of Hopf fibration. Reprinted with permission from Ref. [67]. Copyright 2013 American Physical Society. (**d**) Self-assembly of skyrmions. Reprinted with permission from Ref. [77]. Copyright 2015 Nature. (**e**) Knotted co-located half-integer vortex lines in a heliknoton. (**f**) Polarizing microscopy texture of heliknotons. Reprinted with permission from Ref. [82]. Copyright 2019 Science.

In most investigations, these topological solitons are viewed as static field configurations in LCs. However, it is found that they can be driven into motion by applying electric fields. In 2017, Ackerman et al. reported an electrically driven squirming motion of baby skyrmions in a chiral nematic [90]. By applying a modulated electric field, the skyrmions behave like defects in active matter and move in directions orthogonal to the electric field. Such a motion stems from the non-reciprocal rotational dynamics of LC director fields. During motion, the periodic relaxation and tightening of the twisted region make the skyrmions expand, contract, and morph, resembling squirming motion (Figure 7a). Both the direction and speed of the moving solitons can be controlled by tuning the applied electric field. Such a controllable motion of skyrmions may enable versatile applications such as micro-cargo transport [91]. In 2019, Sohn et al. reported an electrically driven collective motion of skyrmions, in which thousands to millions of skyrmions started from random orientations and motions, but then synchronized their motions and developed polar ordering within seconds (Figure 7b) [92]. They also showed that such a collective motion could even be enriched and guided by light (Figure 7c) [93] and could be used as a model for studying the dynamics of topological defects and grain boundaries in crystalline solid systems [94]. As we mentioned above, the topological defects and solitons are usually generated through local relief of geometric frustration of the helical structure of CNLCs.

As a result, in most works, the topological defects are generated in CNLCs confined by homeotropic anchoring conditions. Very recently, Shen and Dierking reported the creation of 3D topological solitons, i.e., the torons, in a CNLC which is confined in cells of homogeneous anchoring by applying electric fields [95]. In that work, the authors demonstrate the transformation between the cholesteric fingers and the solitons and the formation of "skyrmion bags" with a tunable topological degree. The solitons exhibit different static geometric textures and dynamic behaviors by changing the pitch of the CNLC system (Figure 7d). They undergo anomalous diffusion at equilibrium and performed directional motion driven by electric fields. The solitons could even form aggregates of tunable shape, anisotropy, and fractal dimension through inelastic collisions with each other.
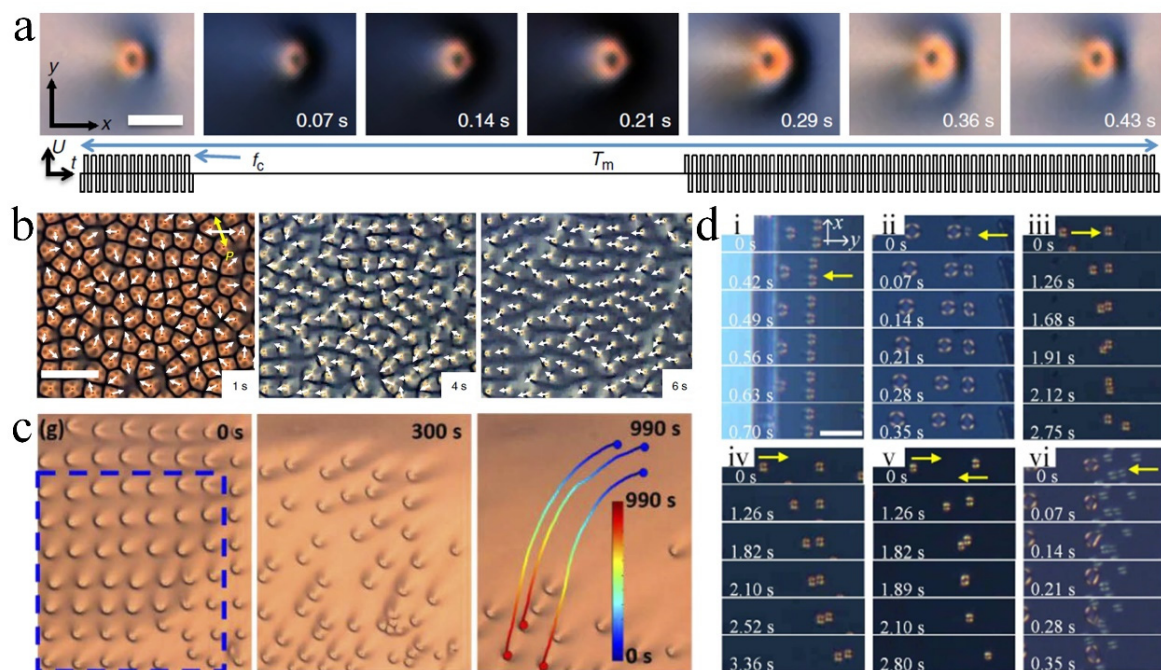
Figure 7. (**a**) Polarizing microscopy texture of a squirming skyrmion. Reprinted with permission from Ref. [90]. Copyright 2017 Nature. (**b**) Temporal evolution of skyrmion velocity order. Reprinted with permission from Ref. [92]. Copyright 2019 Nature. (**c**) Motion of skyrmions guided by light. Reprinted with permission from Ref. [93]. Copyright 2020 Optical Society of America. (**d**) Different dynamic behaviors of torons. Reprinted with permission from Ref. [95]. Copyright 2021 American Physical Society.

In this section, the recent experimental studies on 3D particle-like skyrmionic topological solitons were briefly introduced. For readers who are interested in more details concerning this topic, an excellent review written by Smalyukh is strongly recommended [96].

5. Dynamic Dissipative Solitons in Liquid Crystals

Dissipative solitons are stable localized solitary deviations of a state variable from an otherwise homogeneous stable stationary background distribution. They are generally powered by an external driver and vanish below a finite strength of the driver [97]. Experimentally, dissipative solitons were generated in the form of electric current filaments in a 2D planar gas-discharge system [98]. In LCs, different kinds of dissipative solitons have been generated and reported recently [99–105].

In 2018, Li et al. reported the formation of 3D dissipative solitons in an electrically driven nematic, which were called "director bullets" [99] or "directrons" [100] by the authors (Figure 8). These solitons were first reported by Brand et al. in 1997, and were called "butterflies", but did not receive much attention at that time. The directrons (we will refer to them as "directrons" to distinguish them from other solitons) are self-confined

localized director deformations. While the nematic aligns homogeneously outside the directrons, the director field is distorted and oscillates with the frequency of the applied AC electric field within the directrons. Such an oscillation breaks the fore-aft symmetry of the structure of the directrons and leads to the rapid propagation perpendicular to the alignment direction. The directrons can move with speeds as large as 1000 μm s^{-1} through the homogeneous nematic bulk over a macroscopic distance thousands of times larger than their size. They survive collisions and pass through each other without losing their identities. Unlike the topological solitons, the directrons are topologically equivalent to a uniform state and disappear right after switching off the applied electric field. The nematic media in which the directrons were generated by Li et al., 4'-butyl-4-heptyl-bicyclohexyl-4-carbonitrile (CCN-47), is of the (−,−) type, which means that both the dielectric and conductivity anisotropies are negative, i.e., $\Delta\varepsilon = \varepsilon_{\parallel} - \varepsilon_{\perp} < 0$ and $\Delta\sigma = \sigma_{\parallel} - \sigma_{\perp} < 0$, respectively. The basic mechanism of many electro-hydrodynamic instabilities in nematics of the (−,+) type is now quite well understood and can be explained by the well-known "Carr-Helfrich" model, in which a subtle balance between the dielectric torque that stabilizes the initial planar director field and an anomalous conductive torque induced by space charges that breaks the planar state is reached [106,107]. However, the model cannot be used to explain the generation of the directrons observed in (−,−) nematics, in which case both the dielectric and conductivity torques can only stabilize the planar state. Instead, due to the equality of the frequency of the directron oscillation and that of the applied electric field, the main reason of the excitation of the directrons is attributed to the flexoelectric polarization [105].
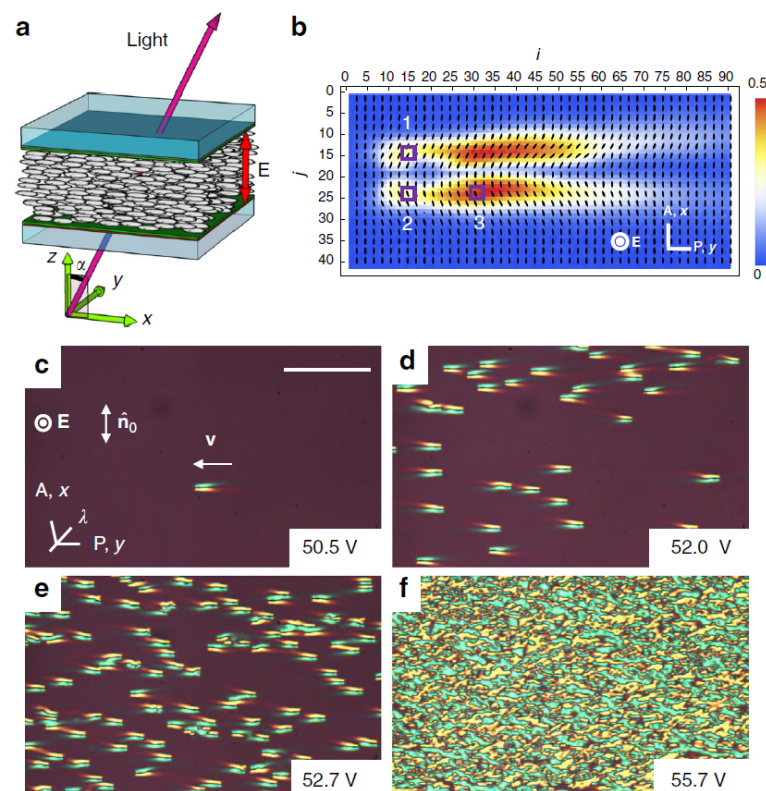

Figure 8. Director bullets in a planar nematic cell. (**a**) Cell scheme. (**b**) Transmitted light intensity map and director distortions in the *xy* plane within a single bullet. (**c–e**) Polarizing microscopy of the director bullets at varied voltages. (**f**) Polarizing microscopy of the electro-hydrodynamic pattern. Scale bar 200 μm. Reprinted with permission from Ref. [99]. Copyright 2018 Nature.

The study carried out by Aya and Araoka showed that similar directrons can also be generated in nematics of the (−,+) type [101]. In order to systemically examine the

influences of the material parameters on the generation and dynamics of the directrons, the authors used a mixture of two different nematics which are of the $(-,-)$ type and the $(+,+)$ type, respectively. By altering the concentrations of the two nematics, a continuous transition of the dielectric and conductivity anisotropies of the mixture could be realized, leading to the formation of different kinds of electro-hydrodynamic patterns. The authors found that the conductivity is vital in determining the stability of the directrons. These directrons can only exist in the limited range of moderate conductivity, $0.8 \times 10^{-8} < \sigma < 4 \times 10^{-8}~\Omega^{-1}\mathrm{m}^{-1}$. The unifying feature of the generation of the directrons in nematics of the $(-,-)$ type and the $(-,+)$ type is that the conductivity of the nematic host is relatively low compared to those typically used in exploring conventional Carr-Helfrich electro-hydrodynamic phenomena ($\sim 10^{-7}~\Omega^{-1}\mathrm{m}^{-1}$) [108]. Li et al. reported that the conductivity of the nematic host (CCN-47) for producing dissipative solitons was about $(0.5–0.6) \times 10^{-8}~\Omega^{-1}\mathrm{m}^{-1}$ [99], and the conductivity of the nematic (ZLI-2806) used in the experiments by Shen and Dierking was about $(0.6–1.9) \times 10^{-8}~\Omega^{-1}\mathrm{m}^{-1}$ [102].

On the other hand, a recent study carried out by Shen and Dierking showed that similar directrons could even be produced in nematics of the $(+,+)$ type (Figure 9) [103], which is unexpected by the "standard model" [109]. In their experiment, a nematic (5CB) with both positive dielectric and conductivity anisotropies was confined in a cell with homogeneous alignment. The alignment of the cells was induced through the photo-alignment technique instead of the conventional rubbing method, the former providing a relatively weak azimuthal anchoring. The directrons are generated after applying an AC electric field with a relatively low frequency to the sample. The dynamic behavior of the directrons is similar to that reported by Li et al. [87,88] and Aya et al. [89]. Directrons can propagate either parallel or perpendicular to the alignment direction which can be switched by tuning the frequency and amplitude of the applied electric field [99–101]. The directrons behave like waves when they pass through each other without losing their identities after collisions. Electro-hydrodynamic instabilities in LCs have been investigated for decades. Early studies mainly focus on the electro-convection effects in nematics with opposite signs of anisotropies, e.g., nematics of the $(-,+)$ type, in which electro-convection rolls, such as the well-known "Williams domains" [110] and "chevrons" [28], are observed. In most of the cases, the destabilization can be explained by the charge separation mechanism introduced by Carr [106] and Helfrich [107], which was later extended to a 3D theory, i.e., the "standard model" [109]. On the other hand, most nonstandard electro-convection phenomena observed in nematics of the $(-,-)$ type can be explained by adding flexoelectricity effects to the standard model. The standard model predicts no electro-hydrodynamic instability in nematics of the $(+,+)$ type. However, complicated electro-convection patterns, such as fingerprint textures [111], Maltese crosses [111], and cellular patterns [112], were reported in nematic cells with homeotropic alignment. Different explanations, including isotropic ionic flows [111,113,114], charge injection (known as Felici-Benard mechanism) [115,116], flexoelectricity, and surface-polarization effects [117,118], etc., were proposed to account for the origin of the instabilities. However, a rigorous explanation is still to be found. In the case of homogeneous alignment, only stationary Williams domains were observed in nematics with small values of the dielectric anisotropy ($0 < \Delta\varepsilon < 0.4$). For nematics with large dielectric anisotropy (just as the situation in ref [103]), electro-hydrodynamic instabilities are usually suppressed by the Freedericksz transition and thus are not expected [119]. The formation of the directrons in 5CB reported by Shen and Dierking is attributed to the special conditions of their experimental setup, i.e., a relatively high ion concentration of the nematic host and a relatively weak azimuthal anchoring of the cells. Both of these factors lead to the strong nonlinear coupling between the isotropic ionic flows and the director field which induces the directrons [103].
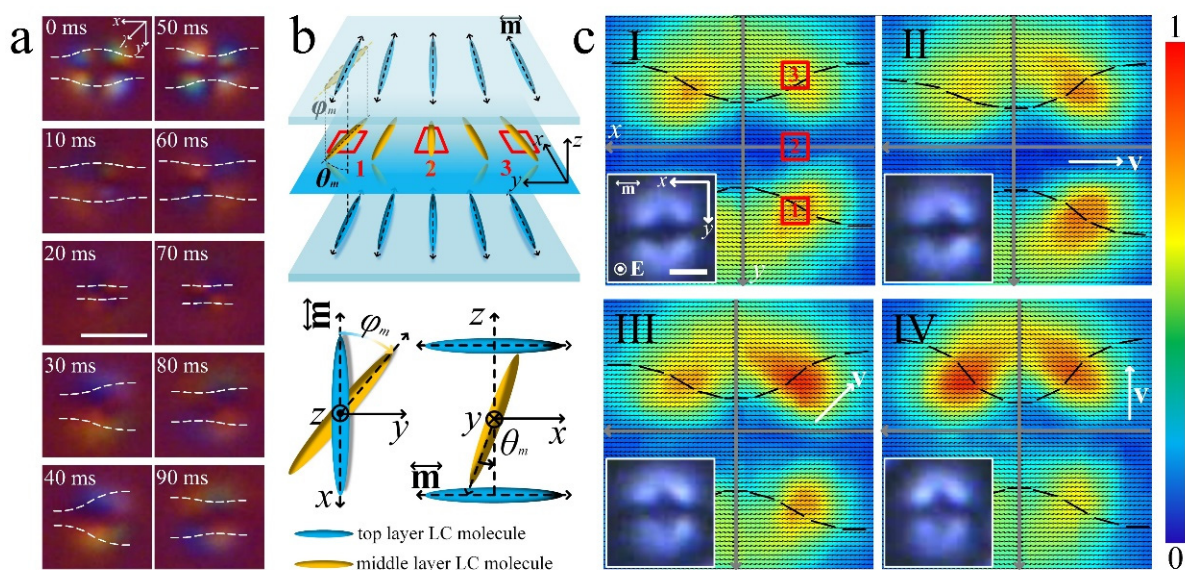
Figure 9. The structure of the dissipative solitons in 5CB. (**a**) Time series of polarizing micrographs of a soliton modulated by an AC electric field. Scale bar 20 μm. (**b**) The schematic structure of a soliton. **m** represents the alignment direction. φ_m and θ_m represent the azimuthal angle and the polar angle of the local mid-layer director. (**c**) Transmitted light intensity maps and the corresponding mid-layer director fields (black dashed lines) in the xy plane within solitons. **v** represents the velocity of the soliton. The color bar shows a linear scale of transmitted light intensity. Insets are the corresponding POM micrographs, scale bar 10 μm. Red squares 1, 2, and 3 are corresponding to the ones in (**b**). Reprinted with permission from Ref. [103]. Copyright 2020 Royal Society of Chemistry.

The formation of the dynamic directrons is not the privilege of nematics only. Shen and Dierking showed that the directrons can also form in chiral nematics of the $(-,+)$ type and the $(+,+)$ type, respectively [102,103]. In the experiments, the chiral nematic hosts are prepared by doping a chiral dopant into achiral nematics, and the mixtures are filled into LC cells with homogeneous alignment conditions. An AC electric field is applied parallel to the helical axis of the chiral nematics, and the directrons emerge as the amplitude of the electric field increases above some frequency-dependent thresholds. The dynamic behavior of the directrons was investigated and compared to those in achiral nematics. It was found that the directrons in the achiral nematics show a "butterfly-like" structure (Figure 10a), but the ones in chiral nematics exhibit a "bullet-like" structure (Figure 10b). In both cases (chiral and achiral nematics), the directrons move either parallel or perpendicular to the alignment direction, a behavior which is dependent on the applied electric field. Interestingly, the directrons in achiral nematics behave like waves in that they collide and pass through each other as reported by Li et al. [99]. The directrons in chiral nematics behave similar to a wave-particle dualism in so far that they either pass through each other without losing identity (solitary wave) (Figure 10c), or collide with each other and undergo reflection (hard particle) (Figure 10d). The authors also showed that the motion of the directrons can be controlled by the alignment. As shown in Figure 10e, the LC cell is divided into three regions with different alignment directions by using the photo-alignment technique. Tuning the applied electric field, the directrons either move parallel or perpendicular to the alignment direction in each individual region. However, once the directrons move across the boundaries of different regions, they change their directions continuously to fit the alignment condition. The directrons can therefore be used as vehicles for micro-cargo transport [102,103]. As shown in Figure 10f, a directron is induced around a dust particle once the electric field is applied. It then carries and translates the particle by moving it through the nematic bulk. Similar phenomena were also reported by Li et al. which was termed "directron-induced liquid crystal-enabled electrophoresis" [120].
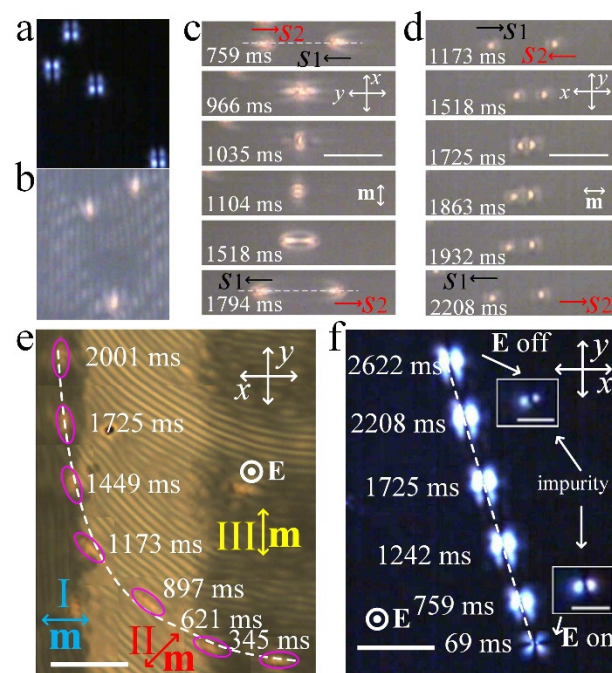
Figure 10. Dissipative solitons in chiral nematics. Solitons in achiral (**a**) and chiral (**b**) nematics. (**c**) Two solitons pass through each other. (**d**) Two solitons collide and reflect into opposite directions. (**e**) Motion of solitons in a cell divided into three regions with different alignment directions. (**f**) Micro-cargo transport by a soliton. Reprinted with permission from Ref. [102]. Copyright 2020 Nature.

So far, most dynamic solitons have been reported only in nematics. However, recently, it was shown that particle-like dynamic dissipative solitons can be formed in LCs of the fluid smectic A phase [104]. A smectic A phase is characterized by the formation of a layered structure of elongated molecules with orientational and 1D positional order. Within each layer, the LC molecules are orientated perpendicular to the layer, but their molecular centers of mass are distributed randomly without any further in-plane positional order [121]. The smectic phase is usually characterized by the remarkable patterns of singular ellipses, hyperbolas, and parabolas known as the focal conic domains (FCDs). In this work, a smectic LC (8CB) is confined in a LC cell with homogeneous alignment condition. The sample is kept at a temperature slightly below the nematic-smectic phase transition point. The solitons are formed by applying a low-frequency field with a mediate voltage to the so-called "scattering state" of the smectic A phase. The solitons exhibit a swallow-tail like texture under crossed polarizers with a static structure analogous to the parabolic focal conic domains (PFCDs) (Figure 11). They are characterized by an elliptical contour, which is generated as a result of the localization of stress. The contour is composed of the loci of the cusps of smectic layers. Outside the solitons, the equidistant smectic layers align homogeneously perpendicular to the alignment direction. Within the solitons, the transmitted light intensity increases, indicating azimuthal deviations of the director field from the alignment. As a result, the smectic layers continuously deform into curves within the solitons. The curvature of the curves exhibits a maximum at one of the foci of the elliptical contour, where a singular defect line is located and acts as the core of the solitons. The size of the solitons is dependent on the applied voltage, and decreases with increasing voltage. When driven by a low-frequency electric field, the director within the solitons tilts up and down due to the dielectric torque, which leads to a periodic shape transformation of the soliton. The solitons move bidirectionally along the alignment direction with constant speed, which is attributed to the permeation ion flow perpendicular to the smectic layers. The solitons behave like particles when they collide with each other. They can also interact with colloidal micro-particles.
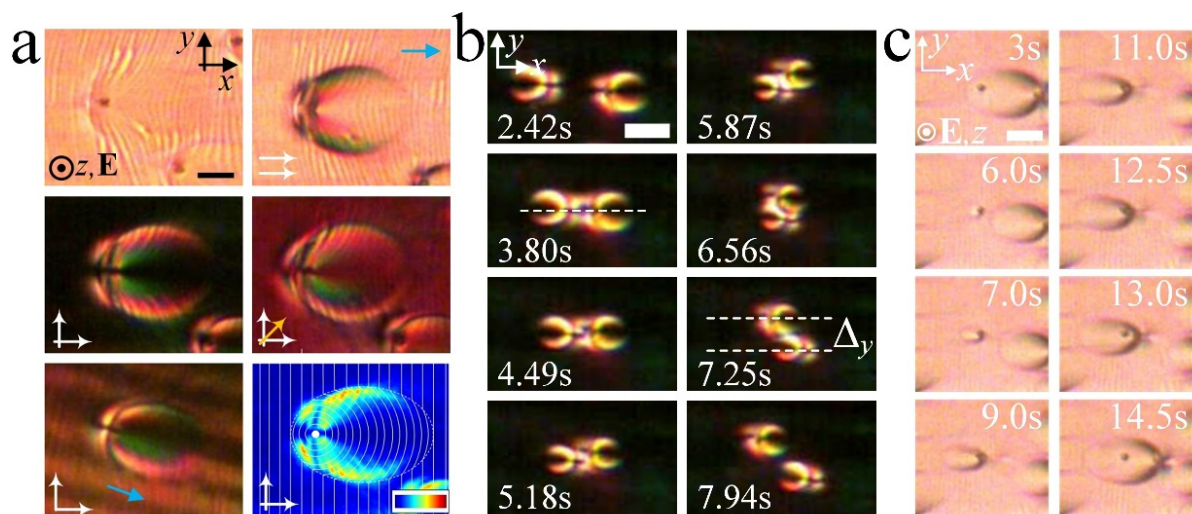
Figure 11. Swallow-tail solitons in smectics. (**a**) Polarizing micrographs of the swallow-tail soliton and its corresponding static structure. (**b**) Collision of two swallow-tail solitons. (**c**) Nucleation of swallow-tail solitons on a colloidal micro-particle. Reprinted with permission from Ref. [104]. Copyright 2021 Royal Society of Chemistry.

6. Conclusions

In summary, we have briefly discussed some important early works of solitons in LCs and the recent progresses made in the investigations of topological solitons and dissipative solitons in LCs. Although recent studies of topological solitons and dissipative solitons have received great attention, many fundamental questions remain unanswered. For instance, the existence of topological solitons with higher dimensions in biaxial liquid crystal systems, a systematic classification of the topological solitons, the stability of the topological and dissipative solitons, the transformation between different topological solitons, the influence of the topological structure on the dynamics and interactions of topological solitons, the formation mechanism of the directrons, the role of ions played in the formation and motion of dissipative solitons, the influence of surface anchoring on the stability, formation and dynamics of the solitons, the effect of chirality on the structure and dynamics of the solitons, the interactions between solitons and colloidal particles, the self-assembly and collective behavior of the solitons, the existence of topological and dissipative soliton in lyotropic and active LC systems, the relation between the solitons in LCs and the solitons in other physical systems, etc. All these questions remain elusive and require further experimental and theoretical investigations to answer.

After over five decades of research, various solitons have been created and described in different liquid crystalline systems. This not only broadens the research and understanding of LCs, but also enhances our understanding of solitons in other physical systems. Furthermore, the solitons in LCs may even lead to novel phenomena, such as emergent collective motion of solitons [92,93], and applications, such as micro-cargo transport [102,103,120], optic processing [84,85], or fast LC displays [14]. We hope this brief review can arouse more researchers' interest in the field of solitons in LC systems.

Author Contributions: Y.S. conceived and wrote the manuscript. I.D. contributed through discussing and writing the manuscript. All authors have read and agreed to the published version of the manuscript.

Institutional Review Board Statement: Not applicable.

Informed Consent Statement: Not applicable.

Data Availability Statement: Not applicable.

Conflicts of Interest: The authors declare no conflict of interest.

References

1. Russell, J.S. *Report on Waves: Made to the Meetings of the British Association in 1842–1843*; Richard and John E Taylor: London, UK, 1845.
2. Korteweg, D.J.; De Vries, G. XLI. On the change of form of long waves advancing in a rectangular canal, and on a new type of long stationary waves. *Lond. Edinb. Dublin Philos. Mag. J. Sci.* **1895**, *39*, 422–443. [CrossRef]
3. Zabusky, N.J.; Kruskal, M.D. Interaction of "Solitons" in a Collisionless Plasma and the Recurrence of Initial States. *Phys. Rev. Lett.* **1965**, *15*, 240–243. [CrossRef]
4. Du, L.; Yang, A.; Zayats, A.V.; Yuan, X. Deep-subwavelength features of photonic skyrmions in a confined electromagnetic field with orbital angular momentum. *Nat. Phys.* **2019**, *15*, 650–654. [CrossRef]
5. Ray, M.W.; Ruokokoski, E.; Kandel, S.; Möttönen, M.; Hall, D. Observation of Dirac monopoles in a synthetic magnetic field. *Nature* **2014**, *505*, 657–660. [CrossRef]
6. Harada, K.; Matsuda, T.; Bonevich, J.; Igarashi, M.; Kondo, S.; Pozzi, G.; Kawabe, U.; Tonomura, A. Real-time observation of vortex lattices in a superconductor by electron microscopy. *Nature* **1992**, *360*, 51–53. [CrossRef]
7. Yu, X.; Onose, Y.; Kanazawa, N.; Park, J.; Han, J.; Matsui, Y.; Nagaosa, N.; Tokura, Y. Real-space observation of a two-dimensional skyrmion crystal. *Nature* **2010**, *465*, 901–904. [CrossRef] [PubMed]
8. Scott, A.C.; Chu, F.Y.F.; McLaughlin, D.W. The soliton: A new concept in applied science. *Proc. IEEE* **1973**, *61*, 1443–1483. [CrossRef]
9. Bullough, R. Solitons. *Phys. Bull.* **1978**, *29*, 78. [CrossRef]
10. Malomed, B.A.; Mihalache, D.; Wise, F.; Torner, L. Spatiotemporal optical solitons. *J. Opt. B Quantum Semiclassical Opt.* **2005**, *7*, R53. [CrossRef]
11. Dauxois, T.; Peyrard, M. *Physics of Solitons*; Cambridge University Press: Cambridge, UK, 2006.
12. De Gennes, P.-G.; Prost, J. *The Physics of Liquid Crystals*, 2nd ed.; Oxford University Press: Oxford, UK, 1993; Volume 83.
13. Shen, Y.; Dierking, I. Perspectives in Liquid-Crystal-Aided Nanotechnology and Nanoscience. *Appl. Sci.* **2019**, *9*, 2512. [CrossRef]
14. Lam, L.; Prost, J. *Solitons in Liquid Crystals*; Springer Science & Business Media: New York, NY, USA, 2012.
15. Helfrich, W. Alignment-Inversion Walls in Nematic Liquid Crystals in the Presence of a Magnetic Field. *Phys. Rev. Lett.* **1968**, *21*, 1518–1521. [CrossRef]
16. De Gennes, P. Mouvements de parois dans un nématique sous champ tournant. *J. De Phys.* **1971**, *32*, 789–792. [CrossRef]
17. Leger, L. Observation of wall motions in nematics. *Solid State Commun.* **1972**, *10*, 697–700. [CrossRef]
18. Brochard, F. Mouvements de parois dans une lame mince nématique. *J. De Phys.* **1972**, *33*, 607–611. [CrossRef]
19. Leger, L. Static and dynamic behaviour of walls in nematics above a Freedericks transition. *Solid State Commun.* **1972**, *11*, 1499–1501. [CrossRef]
20. Léger, L. Walls in Nematics. *Mol. Cryst. Liq. Cryst.* **1973**, *24*, 33–44. [CrossRef]
21. Shen, Y.; Dierking, I. Annihilation dynamics of reverse tilt domains in nematic liquid crystals. *J. Mol. Liq.* **2020**, *313*, 113547. [CrossRef]
22. Cladis, P.; Torza, S. Flow instabilities in Couette flow in nematic liquid crystals. In *Hydrosols and Rheology*; Elsevier: London, UK, 1976; pp. 487–499.
23. Guozhen, Z. Experiments on Director Waves in Nematic Liquid Crystals. *Phys. Rev. Lett.* **1982**, *49*, 1332–1335. [CrossRef]
24. Lei, L.; Changqing, S.; Juelian, S.; Lam, P.M.; Yun, H. Soliton Propagation in Liquid Crystals. *Phys. Rev. Lett.* **1982**, *49*, 1335–1338. [CrossRef]
25. Lei, L.; Changqing, S.; Gang, X. Generation and detection of propagating solitons in shearing liquid crystals. *J. Stat. Phys.* **1985**, *39*, 633–652. [CrossRef]
26. Lin, L.; Shu, C.; Xu, G. Comment on "on solitary waves in liquid crystals". *Phys. Lett. A* **1985**, *109*, 277–278. [CrossRef]
27. Shu, C.Q.; Shao, R.F.; Zheng, S.; Liang, Z.C.; He, G.; Xu, G.; Lam, L. Two-dimensional axisymmetric solitons in nematic liquid crystals. *Liq. Cryst.* **1987**, *2*, 717–722. [CrossRef]
28. Ribotta, R. Critical Behavior of the Penetration Length of a Vortex into a Subcritical Region. *Phys. Rev. Lett.* **1979**, *42*, 1212–1215. [CrossRef]
29. Lowe, M.; Gollub, J.P. Solitons and the commensurate-incommensurate transition in a convecting nematic fluid. *Phys. Rev. A* **1985**, *31*, 3893–3897. [CrossRef] [PubMed]
30. Joets, A.; Ribotta, R. Localized bifurcations and defect instabilities in the convection of a nematic liquid crystal. *J. Stat. Phys.* **1991**, *64*, 981–1005. [CrossRef]
31. Joets, A.; Ribotta, R. Localized, Time-Dependent State in the Convection of a Nematic Liquid Crystal. *Phys. Rev. Lett.* **1988**, *60*, 2164–2167. [CrossRef]
32. Braun, E.; Faucheux, L.; Libchaber, A.; McLaughlin, D.; Muraki, D.; Shelley, M. Filamentation and undulation of self-focused laser beams in liquid crystals. *EPL (Europhys. Lett.)* **1993**, *23*, 239. [CrossRef]

33. Braun, E.; Faucheux, L.P.; Libchaber, A. Strong self-focusing in nematic liquid crystals. *Phys. Rev. A* **1993**, *48*, 611. [CrossRef]
34. Laudyn, U.A.; Kwaśny, M.; Karpierz, M.A.; Assanto, G. Electro-optic quenching of nematicon fluctuations. *Opt. Lett.* **2019**, *44*, 167–170. [CrossRef]
35. Assanto, G. *Nematicons: Spatial Optical Solitons in Nematic Liquid Crystals*; John Wiley & Sons: Hoboken, NJ, USA, 2012; Volume 74.
36. Izdebskaya, Y.V.; Shvedov, V.G.; Jung, P.S.; Krolikowski, W. Stable vortex soliton in nonlocal media with orientational nonlinearity. *Opt. Lett.* **2018**, *43*, 66–69. [CrossRef]
37. Laudyn, U.A.; Kwaśny, M.; Karpierz, M.A.; Assanto, G. Vortex nematicons in planar cells. *Opt. Express* **2020**, *28*, 8282–8290. [CrossRef]
38. Izdebskaya, Y.; Assanto, G.; Krolikowski, W. Observation of stable-vector vortex solitons. *Opt. Lett.* **2015**, *40*, 4182–4185. [CrossRef]
39. Assanto, G.; Karpierz, M.A. Nematicons: Self-localised beams in nematic liquid crystals. *Liq. Cryst.* **2009**, *36*, 1161–1172. [CrossRef]
40. Peccianti, M.; Assanto, G. Nematicons. *Phys. Rep.* **2012**, *516*, 147–208. [CrossRef]
41. Assanto, G. Nematicons: Reorientational solitons from optics to photonics. *Liq. Cryst. Rev.* **2018**, *6*, 170–194. [CrossRef]
42. Manton, N.; Sutcliffe, P. *Topological Solitons*; Cambridge University Press: Cambridge, UK, 2004.
43. Kauffman, L.H. *Knots and Physics*; World Scientific: Farrer Road, Singapore, 2001; Volume 1.
44. Hopf, H. Über die Abbildungen der dreidimensionalen Sphäre auf die Kugelfläche. *Math. Ann.* **1931**, *104*, 637–665. [CrossRef]
45. Finkelstein, D. Kinks. *J. Math. Phys.* **1966**, *7*, 1218–1225. [CrossRef]
46. Shuryak, E.V. The role of instantons in quantum chromodynamics:(I). *Physical vacuum. Nucl. Phys. B* **1982**, *203*, 93–115. [CrossRef]
47. Shuryak, E.V. The role of instantons in quantum chromodynamics:(II). *Hadronic structure. Nucl. Phys. B* **1982**, *203*, 116–139.
48. Abrikosov, A.A. Nobel Lecture: Type-II superconductors and the vortex lattice. *Rev. Mod. Phys.* **2004**, *76*, 975–979. [CrossRef]
49. O'dell, D.; Giovanazzi, S.; Kurizki, G. Rotons in gaseous Bose-Einstein condensates irradiated by a laser. *Phys. Rev. Lett.* **2003**, *90*, 110402. [CrossRef]
50. Skyrme, T.H.R. A unified field theory of mesons and baryons. *Nucl. Phys.* **1962**, *31*, 556–569. [CrossRef]
51. Oswald, P.; Baudry, J.; Pirkl, S. Static and dynamic properties of cholesteric fingers in electric field. *Phys. Rep.* **2000**, *337*, 67–96. [CrossRef]
52. Haas, W.E.L.; Adams, J.E. New optical storage mode in liquid crystals. *Appl. Phys. Lett.* **1974**, *25*, 535–537. [CrossRef]
53. Kawachi, M.; Kogure, O.; Kato, Y. Bubble domain texture of a liquid crystal. *Jpn. J. Appl. Phys.* **1974**, *13*, 1457. [CrossRef]
54. Haas, W.E.L.; Adams, J.E. Electrically variable diffraction in spherulitic liquid crystals. *Appl. Phys. Lett.* **1974**, *25*, 263–264. [CrossRef]
55. Nawa, N.; Nakamura, K. Observation of Forming Process of Bubble Domain Texture in Liquid Crystals. *Jpn. J. Appl. Phys.* **1978**, *17*, 219. [CrossRef]
56. Stieb, A. Structure of elongated and spherulitic domains in long pitch cholesterics with homeotropic boundary alignment. *J. De Phys.* **1980**, *41*, 961–969. [CrossRef]
57. Hirata, S.; Akahane, T.; Tako, T. New Molecular Alignment Models of Bubble Domains and Striped Domains in Cholesteric-Nematic Mixtures. *Mol. Cryst. Liq. Cryst.* **1981**, *75*, 47–67. [CrossRef]
58. Kerllenevich, B.; Coche, A. Bubble domain in cholesteric liquid crystals. *Mol. Cryst. Liq. Cryst.* **1981**, *68*, 47–55. [CrossRef]
59. Bouligand, Y.; Livolant, F. The organization of cholesteric spherulites. *J. De Phys.* **1984**, *45*, 1899–1923. [CrossRef]
60. Pirkl, S.; Ribière, P.; Oswald, P. Forming process and stability of bubble domains in dielectrically positive cholesteric liquid crystals. *Liq. Cryst.* **1993**, *13*, 413–425. [CrossRef]
61. Pirkl, S.; Oswald, P. From bubble domains to spirals in cholesteric liquid crystals. *J. De Phys. II* **1996**, *6*, 355–373. [CrossRef]
62. Baudry, J.; Pirkl, S.; Oswald, P. Looped finger transformation in frustrated cholesteric liquid crystals. *Phys. Rev. E* **1999**, *59*, 5562–5571. [CrossRef] [PubMed]
63. Smalyukh, I.I.; Lansac, Y.; Clark, N.A.; Trivedi, R.P. Three-dimensional structure and multistable optical switching of triple-twisted particle-like excitations in anisotropic fluids. *Nat. Mater.* **2009**, *9*, 139. [CrossRef] [PubMed]
64. Trushkevych, O.; Ackerman, P.; Crossland, W.A.; Smalyukh, I.I. Optically generated adaptive localized structures in confined chiral liquid crystals doped with fullerene. *Appl. Phys. Lett.* **2010**, *97*, 201906. [CrossRef]
65. Ackerman, P.J.; Qi, Z.; Smalyukh, I.I. Optical generation of crystalline, quasicrystalline, and arbitrary arrays of torons in confined cholesteric liquid crystals for patterning of optical vortices in laser beams. *Phys. Rev. E* **2012**, *86*, 021703. [CrossRef]
66. Smalyukh, I.I.; Kaputa, D.; Kachynski, A.V.; Kuzmin, A.N.; Ackerman, P.J.; Twombly, C.W.; Lee, T.; Trivedi, R.P.; Prasad, P.N. Optically generated reconfigurable photonic structures of elastic quasiparticles in frustrated cholesteric liquid crystals. *Opt. Express* **2012**, *20*, 6870–6880. [CrossRef] [PubMed]
67. Chen, B.G.-G.; Ackerman, P.J.; Alexander, G.P.; Kamien, R.D.; Smalyukh, I.I. Generating the Hopf fibration experimentally in nematic liquid crystals. *Phys. Rev. Lett.* **2013**, *110*, 237801. [CrossRef]
68. Ackerman, P.J.; Trivedi, R.P.; Senyuk, B.; van de Lagemaat, J.; Smalyukh, I.I. Two-dimensional skyrmions and other solitonic structures in confinement-frustrated chiral nematics. *Phys. Rev. E* **2014**, *90*, 012505. [CrossRef]
69. Ackerman, P.J.; Smalyukh, I.I. Diversity of Knot Solitons in Liquid Crystals Manifested by Linking of Preimages in Torons and Hopfions. *Phys. Rev. X* **2017**, *7*, 011006. [CrossRef]

70. Ackerman, P.J.; Smalyukh, I.I. Reversal of helicoidal twist handedness near point defects of confined chiral liquid crystals. *Phys. Rev. E* **2016**, *93*, 052702. [CrossRef]
71. Nych, A.; Fukuda, J.-i.; Ognysta, U.; Žumer, S.; Muševič, I. Spontaneous formation and dynamics of half-skyrmions in a chiral liquid-crystal film. *Nat. Phys.* **2017**, *13*, 1215. [CrossRef]
72. Fukuda, J.-I.; Nych, A.; Ognysta, U.; Žumer, S.; Muševič, I. Liquid-crystalline half-Skyrmion lattice spotted by Kossel diagrams. *Sci. Rep.* **2018**, *8*, 1–8. [CrossRef]
73. Duzgun, A.; Nisoli, C. Artificial spin ice of liquid crystal skyrmions. *arXiv* **2019**, arXiv:1908.03246.
74. Foster, D.; Kind, C.; Ackerman, P.J.; Tai, J.-S.B.; Dennis, M.R.; Smalyukh, I.I. Two-dimensional skyrmion bags in liquid crystals and ferromagnets. *Nat. Phys.* **2019**. [CrossRef]
75. Pandey, M.B.; Porenta, T.; Brewer, J.; Burkart, A.; Čopar, S.; Žumer, S.; Smalyukh, I.I. Self-assembly of skyrmion-dressed chiral nematic colloids with tangential anchoring. *Phys. Rev. E* **2014**, *89*, 060502. [CrossRef] [PubMed]
76. Porenta, T.; Čopar, S.; Ackerman, P.J.; Pandey, M.B.; Varney, M.C.M.; Smalyukh, I.I.; Žumer, S. Topological Switching and Orbiting Dynamics of Colloidal Spheres Dressed with Chiral Nematic Solitons. *Sci. Rep.* **2014**, *4*, 7337. [CrossRef]
77. Ackerman, P.J.; van de Lagemaat, J.; Smalyukh, I.I. Self-assembly and electrostriction of arrays and chains of hopfion particles in chiral liquid crystals. *Nat. Commun.* **2015**, *6*, 6012. [CrossRef]
78. Kim, Y.H.; Gim, M.-J.; Jung, H.-T.; Yoon, D.K. Periodic arrays of liquid crystalline torons in microchannels. *RSC Adv.* **2015**, *5*, 19279–19283. [CrossRef]
79. Sohn, H.R.O.; Liu, C.D.; Wang, Y.; Smalyukh, I.I. Light-controlled skyrmions and torons as reconfigurable particles. *Opt. Express* **2019**, *27*, 29055–29068. [CrossRef]
80. Ackerman, P.J.; Smalyukh, I.I. Static three-dimensional topological solitons in fluid chiral ferromagnets and colloids. *Nat. Mater.* **2016**, *16*, 426. [CrossRef]
81. Tai, J.-S.B.; Ackerman, P.J.; Smalyukh, I.I. Topological transformations of Hopf solitons in chiral ferromagnets and liquid crystals. *Proc. Natl. Acad. Sci. USA* **2018**, *115*, 921. [CrossRef] [PubMed]
82. Tai, J.-S.B.; Smalyukh, I.I. Three-dimensional crystals of adaptive knots. *Science* **2019**, *365*, 1449. [CrossRef]
83. Varanytsia, A.; Chien, L.-C. Photoswitchable and dye-doped bubble domain texture of cholesteric liquid crystals. *Opt. Lett.* **2015**, *40*, 4392–4395. [CrossRef] [PubMed]
84. Hess, A.J.; Poy, G.; Tai, J.-S.B.; Žumer, S.; Smalyukh, I.I. Control of light by topological solitons in soft chiral birefringent media. *Phys. Rev. X* **2020**, *10*, 031042. [CrossRef]
85. Poy, G.; Hess, A.J.; Smalyukh, I.I.; Žumer, S. Chirality-enhanced periodic self-focusing of light in soft birefringent media. *Phys. Rev. Lett.* **2020**, *125*, 077801. [CrossRef] [PubMed]
86. Loussert, C.; Iamsaard, S.; Katsonis, N.; Brasselet, E. Subnanowatt Opto-Molecular Generation of Localized Defects in Chiral Liquid Crystals. *Adv. Mater.* **2014**, *26*, 4242–4246. [CrossRef]
87. Varanytsia, A.; Chien, L.-C. P-134: A Spatial Light Modulator with a Two-Dimensional Array of Liquid Crystal Bubbles. *SID Symp. Dig. Tech. Pap.* **2014**, *45*, 1492–1495. [CrossRef]
88. Papič, M.; Mur, U.; Zuhail, K.P.; Ravnik, M.; Muševič, I.; Humar, M. Topological liquid crystal superstructures as structured light lasers. *Proc. Natl. Acad. Sci. USA* **2021**, *118*, 1–7. [CrossRef]
89. Mai, Z.; Yuan, Y.; Tai, J.-S.B.; Senyuk, B.; Liu, B.; Li, H.; Wang, Y.; Zhou, G.; Smalyukh, I.I. Nematic Order, Plasmonic Switching and Self-Patterning of Colloidal Gold Bipyramids. *Adv. Sci.* **2021**, *8*, 2102854. [CrossRef]
90. Ackerman, P.J.; Boyle, T.; Smalyukh, I.I. Squirming motion of baby skyrmions in nematic fluids. *Nat. Commun.* **2017**, *8*, 673. [CrossRef]
91. Sohn, H.R.O.; Ackerman, P.J.; Boyle, T.J.; Sheetah, G.H.; Fornberg, B.; Smalyukh, I.I. Dynamics of topological solitons, knotted streamlines, and transport of cargo in liquid crystals. *Phys. Rev. E* **2018**, *97*, 052701. [CrossRef]
92. Sohn, H.R.O.; Liu, C.D.; Smalyukh, I.I. Schools of skyrmions with electrically tunable elastic interactions. *Nat. Commun.* **2019**, *10*, 4744. [CrossRef] [PubMed]
93. Sohn, H.R.; Liu, C.D.; Voinescu, R.; Chen, Z.; Smalyukh, I.I. Optically enriched and guided dynamics of active skyrmions. *Opt. Express* **2020**, *28*, 6306–6319. [CrossRef]
94. Sohn, H.R.; Smalyukh, I.I. Electrically powered motions of toron crystallites in chiral liquid crystals. *Proc. Natl. Acad. Sci. USA* **2020**, *117*, 6437-6445. [CrossRef] [PubMed]
95. Shen, Y.; Dierking, I. Electrically Driven Formation and Dynamics of Skyrmionic Solitons in Chiral Nematics. *Phys. Rev. Appl.* **2021**, *15*, 054023. [CrossRef]
96. Smalyukh, I.I. knots and other new topological effects in liquid crystals and colloids. *Rep. Prog. Phys.* **2020**, *83*, 106601. [CrossRef]
97. Purwins, H.-G.; Bödeker, H.; Amiranashvili, S. Dissipative solitons. *Adv. Phys.* **2010**, *59*, 485–701. [CrossRef]
98. Bödeker, H.; Röttger, M.; Liehr, A.; Frank, T.; Friedrich, R.; Purwins, H.-G. Noise-covered drift bifurcation of dissipative solitons in a planar gas-discharge system. *Phys. Rev. E* **2003**, *67*, 056220. [CrossRef]
99. Li, B.-X.; Borshch, V.; Xiao, R.-L.; Paladugu, S.; Turiv, T.; Shiyanovskii, S.V.; Lavrentovich, O.D. Electrically driven three-dimensional solitary waves as director bullets in nematic liquid crystals. *Nat. Commun.* **2018**, *9*, 2912. [CrossRef]
100. Li, B.-X.; Xiao, R.-L.; Paladugu, S.; Shiyanovskii, S.V.; Lavrentovich, O.D. Three-dimensional solitary waves with electrically tunable direction of propagation in nematics. *Nat. Commun.* **2019**, *10*, 3749. [CrossRef]
101. Aya, S.; Araoka, F. Kinetics of motile solitons in nematic liquid crystals. *Nat. Commun.* **2020**, *11*, 1–10. [CrossRef]

102. Shen, Y.; Dierking, I. Dynamics of electrically driven solitons in nematic and cholesteric liquid crystals. *Commun. Phys.* **2020**, *3*, 1. [CrossRef]

103. Shen, Y.; Dierking, I. Dynamic dissipative solitons in nematics with positive anisotropies. *Soft Matter* **2020**, *16*, 5325. [CrossRef] [PubMed]

104. Shen, Y.; Dierking, I. Electrically driven formation and dynamics of swallow-tail solitons in smectic A liquid crystals. *Mater. Adv.* **2021**. [CrossRef]

105. Lavrentovich, O.D. Design of nematic liquid crystals to control microscale dynamics. *Liq. Cryst. Rev.* **2020**, *8*, 59–129. [CrossRef]

106. Carr, E.F. Influence of Electric Fields on the Molecular Alignment in the Liquid Crystal p-(Anisalamino)-phenyl Acetate. *Mol. Cryst.* **1969**, *7*, 253–268. [CrossRef]

107. Helfrich, W. Conduction-Induced Alignment of Nematic Liquid Crystals: Basic Model and Stability Considerations. *J. Chem. Phys.* **1969**, *51*, 4092–4105. [CrossRef]

108. Ibragimov, T.D. Influence of fullerenes C60 and single-walled carbon nanotubes on the Carr–Helfrich effect in nematic liquid crystal. *Optik* **2021**, *237*, 166768. [CrossRef]

109. Bodenschatz, E.; Zimmermann, W.; Kramer, L. On electrically driven pattern-forming instabilities in planar nematics. *J. De Phys.* **1988**, *49*, 1875–1899. [CrossRef]

110. Smith, I.; Galerne, Y.; Lagerwall, S.; Dubois-Violette, E.; Durand, G. Dynamics of electrohydrodynamic instabilities in nematic liquid crystals. *Le J. De Phys. Colloq.* **1975**, *36*, C1-237–C231-259. [CrossRef]

111. Barnik, M.I.; Blinov, L.M.; Grebenkin, M.F.; Trufanov, A.N. Dielectric Regime of Electrohydrodynamic Instability in Nematic Liquid Crystals. *Mol. Cryst. Liq. Cryst.* **1976**, *37*, 47–56. [CrossRef]

112. Kumar, P.; Heuer, J.; Tóth-Katona, T.; Éber, N.; Buka, Á. Convection-roll instability in spite of a large stabilizing torque. *Phys. Rev. E* **2010**, *81*, 020702. [CrossRef] [PubMed]

113. Barnik, M.; Blinov, L.; Pikin, S.; Trufanov, A. Instability mechanism in the nematic and isotropic phases of liquid crystals with positive dielectric anisotropy. *Sov Phys JETP* **1977**, *45*, 396–398.

114. Trufanov, A.; Barnik, M.; Blinov, L.; Chigrinov, V. Electrohydrodynamic instability in homeotropically oriented layers of nematic liquid crystals. *Sov Phys JETP* **1981**, *53*, 355–361.

115. Nakagawa, M.; Akahane, T. A new type of electrohydrodynamic instability in nematic liquid crystals with positive dielectric anisotropy. *I. The existence of the charge injection and the diffusion current. J. Phys. Soc. Jpn.* **1983**, *52*, 3773–3781.

116. Nakagawa, M.; Akahane, T. A new type of electrohydrodynamic instability in nematic liquid crystals with positive dielectric anisotropy. *II. Theoretical treatment. J. Phys. Soc. Jpn.* **1983**, *52*, 3782–3789. [CrossRef]

117. Monkade, M.; Martinot-Lagarde, P.; Durand, G. Electric polar surface instability in nematic liquid crystals. *EPL (Europhys. Lett.)* **1986**, *2*, 299. [CrossRef]

118. Lavrentovich, O.; Nazarenko, V.; Pergamenshchik, V.; Sergan, V.; Sorokin, V. Surface-polarization electrooptic effect in a nematic liquid crystal. *Sov. Phys. JETP* **1991**, *72*, 431–444.

119. Buka, A.; Éber, N.; Pesch, W.; Kramer, L. *Advances in Sensing with Security Applications*; Golovin, A.A., Nepomnyashchy, A.A., Eds.; Springer: Dordrecht, The Netherlands, 2006; pp. 55–82.

120. Li, B.-X.; Xiao, R.-L.; Shiyanovskii, S.V.; Lavrentovich, O.D. Soliton-induced liquid crystal enabled electrophoresis. *Phys. Rev. Res.* **2020**, *2*, 013178. [CrossRef]

121. Blinov, L.M. *Structure and Properties of Liquid Crystals*; Springer Science & Business Media: Dordrecht, The Netherlands, 2010; Volume 123.